

HandDiffuse: Generative Controllers for Two-Hand Interactions via Diffusion Models

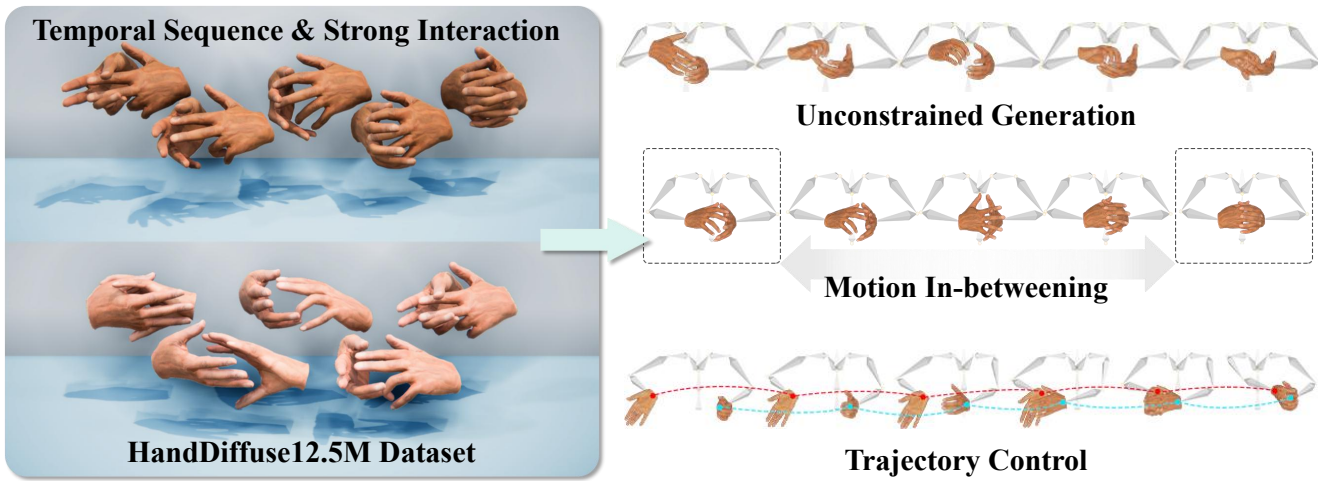
Pei Lin¹Sihang Xu¹Hongdi Yang¹Yiran Liu¹Xin Chen²Jingya Wang¹Jingyi Yu¹Lan Xu¹¹ShanghaiTech University²Tencent PCG<https://handdiffuse.github.io/>

Figure 1. **Overview:** The proposed HandDiffuse12.5M benchmark dataset consists of temporal sequences with strong interaction. Based on HandDiffuse12.5M, we propose HandDiffuse, a strong baseline for the motion generation of interacting hands. HandDiffuse enables three motion generation tasks, including Unconstrained Generation, Motion In-betweening, and Trajectory Control.

Abstract

Existing hands datasets are largely short-range and the interaction is weak due to the self-occlusion and self-similarity of hands, which can not yet fit the need for interacting hands motion generation. To rescue the data scarcity, we propose HandDiffuse12.5M, a novel dataset that consists of temporal sequences with strong two-hand interactions. HandDiffuse12.5M has the largest scale and richest interactions among the existing two-hand datasets. We further present a strong baseline method HandDiffuse for the controllable motion generation of interacting hands using various controllers. Specifically, we apply the diffusion model as the backbone and design two motion representations for different controllers. To reduce artifacts, we also propose Interaction Loss which explicitly quantifies the dynamic interaction process. Our HandDiffuse enables various applications with vivid two-hand interactions, i.e.,

motion in-betweening and trajectory control. Experiments show that our method outperforms the state-of-the-art techniques in motion generation and can also contribute to data augmentation for other datasets. Our dataset, corresponding codes, and pre-trained models will be disseminated to the community for future research towards two-hand interaction modeling.

1. Introduction

The tightly interacting hands play a crucial role in human emotional expression and communication, serving as a vital component for physical interaction with oneself. Controllable hand motion generation not only enhances the experience of augmented reality/virtual reality (AR/VR) but also help robotics and avatars to express their emotion in another dimension.

So far, lots of works have emerged in the field of human body motion generation [4, 22, 51, 59], but the generation of temporal hands motions in strong interaction remains blank as the lack of strong interacting hands datasets. However, the dataset acquisition is time-consuming and expensive due to the interacting hands present self-occlusion, self-similarity, and complex articulations. There are only a few datasets [28, 36, 37, 53, 64] focusing on hands with strong interactions. Most of them, i.e, InterHand2.6M [36], Two-hand 500K [64] and RenderIH [28], provides large-scale discrete frames but the available temporal sequences remain sparse. The severe lack of sufficient temporal motions makes them unsuitable for the motion generation task of two-hand interactions. Only recently, the concurrent work Re:InterHand [37] provides large-scale interaction data, yet it focuses on the motion capture of interacted hands under diverse lighting conditions.

To break the data scarcity, in this paper, we first contribute a comprehensive dataset, *HandDiffuse12.5M*, which focuses on capturing diverse temporal sequences with strong two-hand interactions. Our dataset consists of various modalities, including synchronous 50-view videos, 3D key points, and hand poses. It covers interacting hand motions in random and complex poses, daily communications, finger dances, and Chinese daily sign language with 250k temporal frames, resulting in roughly 12.5 million pictures. To address the issue of occlusion, which is unavoidable in hand interactions, we manually annotate the key points in 240k images. Note that our HandDiffuse12.5M dataset owns the largest scale not only in the number of temporal frames but also in the number of pictures among the existing available interacting hands datasets. Thus, it not only opens up the research for temporally consistent two-hand motion generation but also brings huge potential for future exploration in hand modeling.

Based on our novel dataset, we further provide a strong baseline algorithm named *HandDiffuse*, which tailors the diffusion model [21] to generate vivid interacting hands motions under diverse explicit control. Note that hand motion is an abstract form of emotional expression and ten fingers always gather together during interactions. Therefore, it is difficult to describe the motions with concrete text prompts and the control for motion generation needs to be explicit. To this end, we adopt two kinds of explicit controllers as the conditions for our diffusion models, including the discrete keyframes and the trajectories of wrists. These conditionings enable various downstream applications, ranging from hand motion inbetweening to trajectory-aided hand motion completion which connects hand motions with body motions (see Figure 1). In HandDiffuse, we design two specific motion representations for different controllers, as well as a novel Interaction Loss for the dynamic process of hand interaction, which helps to reduce the artifacts. Finally, we

provide a thorough evaluation of our approach as well as a comparison with state-of-the-art motion generation methods [31, 51]. We also provide results to show that HandDiffuse can contribute to data augmentation for other datasets. Our preliminary outcomes indicate that controllable hand motion generation remains a challenging problem, and our dataset will consistently benefit further investigations of this new research direction. To summarize, our main contributions include:

- We contribute a large-scale dataset, which provides accurate and temporally consistent tracking of human hands under diverse and strong two-hand interactions.
- We propose a strong baseline for generating interacting hand motions from various explicit controllers, enabling vivid motion in-betweening and trajectory conditioning.
- We introduce two motion representations as well as an Interaction Loss to significantly improve the generation results of two-hand interactions.
- Our dataset, related codes, and pre-trained models will be made publicly available to stimulate further research.

2. Related Works

Hand Dataset. The establishment of realistic hand datasets is a challenging and time-consuming process. However, these datasets have significantly accelerated the development of VR/AR, embodied AI and human-object interaction. Many researchers have utilized various sensors, including multiple RGB cameras, depth sensors and maker-base cameras, to collect realistic data in hand-object interaction or dual-hand interaction [3, 5, 9, 11, 13, 15, 17, 18, 27, 34, 36, 37, 40, 47, 48, 53, 57, 58].

Obtaining ground truth for specific dual-hand interaction motion from real-world captured data is challenging [28, 36]. Moon et al. [36] have attempted to combine manual and automated annotations, but manual annotations are labor-intensive. Recently, Moon et al. [37] have improved the detection accuracy of 2D keypoints and reconstructed hands to facilitate fully automated annotation schemes, but these methods are still time-consuming.

As a result, some works have established synthetic hand datasets to enhance annotation precision [10, 28, 32, 63, 64]. Among them, RenderIH [28] increases the diversity of data through re-lighting, while DART [10] provides a wide range of hand accessories to bridge the gap between synthetic and real data. However, synthetic datasets fail to balance the diversity of motion and the continuity of sequences. Some works [28, 64] sample single-frame actions for the left and right hands separately from real datasets and solve the occlusion problem between the hands through optimization. However, such optimization methods are not effective for temporal sequences. Therefore, very few papers [36, 37, 53] have collected temporal interacting hand datasets [28].

Dataset	Temporal Sequence	Source	# Views	Manually Annotation	Appearance
RenderIH [28]	No	Synthesis	-	No	Natural
Two-hand 500K [64]	Partial	IMU+Synthesis	-	No	-
InterHand2.6M [36]	Partial	RGB	80	Yes	Lab
Re:InterHand [37]	Yes	RGB	26	No	Relighting
HandDiffuse12.5M(Ours)	Yes	RGB	50	Yes	Lab

Table 1. **Dataset Comparisons.** We compare our HandDiffuse12.5M dataset with other existing publicly available interacting-hand datasets. Our HandDiffuse12.5M dataset contains both strong interaction and temporal sequences, and has the largest scale.

Hands Capture & Reconstruction. The reconstruction of both hands is a significant challenge in the area of human motion capture [64]. The release of the InterHand2.6M [36] has motivated many regression-based methods [1, 6, 8, 16, 19, 26, 30, 35, 35, 45]. These regression-based methods are widely applied in VTuber and VR/AR devices due to their balance between real-time performance and accuracy. Some works [30, 38] proposed a Transformer-based network with the cross-attention between right and left hands. Recently, Zuo et al. [64] constructed a learning-based prior to capture dual-hands which achieved great results. Building on the impressive performance of diffusion models in image generation [21, 46, 49], DiffHand [29] combines hand reconstruction with diffusion models.

Human Motion generation. In recent years, there has been a growing interest in the field of human motion generation, with many studies exploring the generation of human motions based on conditioning signals. These conditioning signals are used to guide the generation of specific types of motions, such as motion in-betweening [20, 25, 42], trajectory control [24, 43, 54, 60] and unconstrained motion synthesis [39, 55, 62]. Leading by the pioneering work of MDM [52], human motion generation models based on diffusion architecture [7, 31, 61] have been shown to gain better motion diversity and expressiveness compared to prior works based on GAN [33] or VAE [2, 41]. However, most existing works in this area have primarily focused on generating whole-body motions, neglecting the generation of dual-hand motions, which plays a crucial role in many interactive scenarios. Utilizing the capabilities of the diffusion models, we propose a novel method HandDiffuse to enable interacting hands motion generation tasks with control signals such as key frames and trajectory.

3. HandDiffuse1.2M Dataset

3.1. Capture system

Existing hand motion capture solutions include IMU gloves, elastic sensor gloves, marker-based systems, and multi-view camera capture. However, due to the severe occlusion in hand interactions, marker-based systems are not

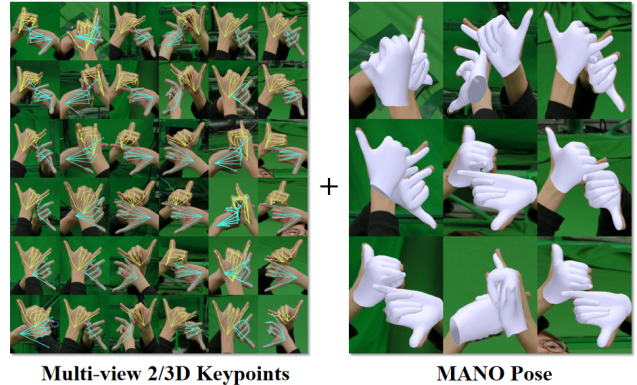


Figure 2. **Overview of our HandDiffuse12.5M.** HandDiffuse12.5M is featured with RGB images, multi-view 2D keypoints, reconstructed 3D keypoints, and MANO [44] parameters.

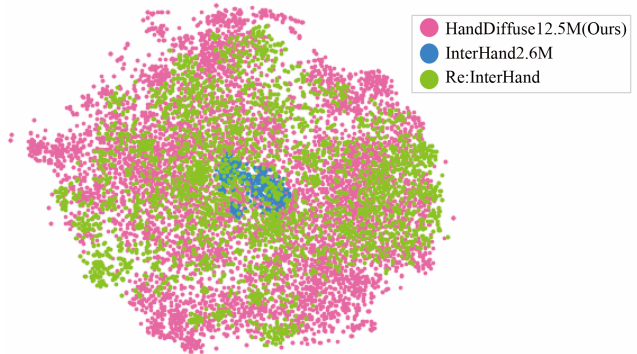


Figure 3. t-SNE visualization of HandDiffuse12.5M(Ours), InterHand2.6M and Re:InterHand. For InterHand2.6M, we only choose its temporal frames. The result indicates the diversity and richness of our HandDiffuse12.5M.

suitable; IMU gloves and elastic sensor-based capture solutions theoretically address the issue of visual occlusion, but these gloves require specific hand shapes from the wearer and are difficult to calibrate in each instance of use. Therefore, we have opted for a multi-view RGB approach combined with manual annotation, similar to InterHand2.6M. As shown in Figure 3, our capture system consists of 50 mounted video cameras (Zcam E2) recording interaction sequences at a frame rate of 30 frames per second (fps). We

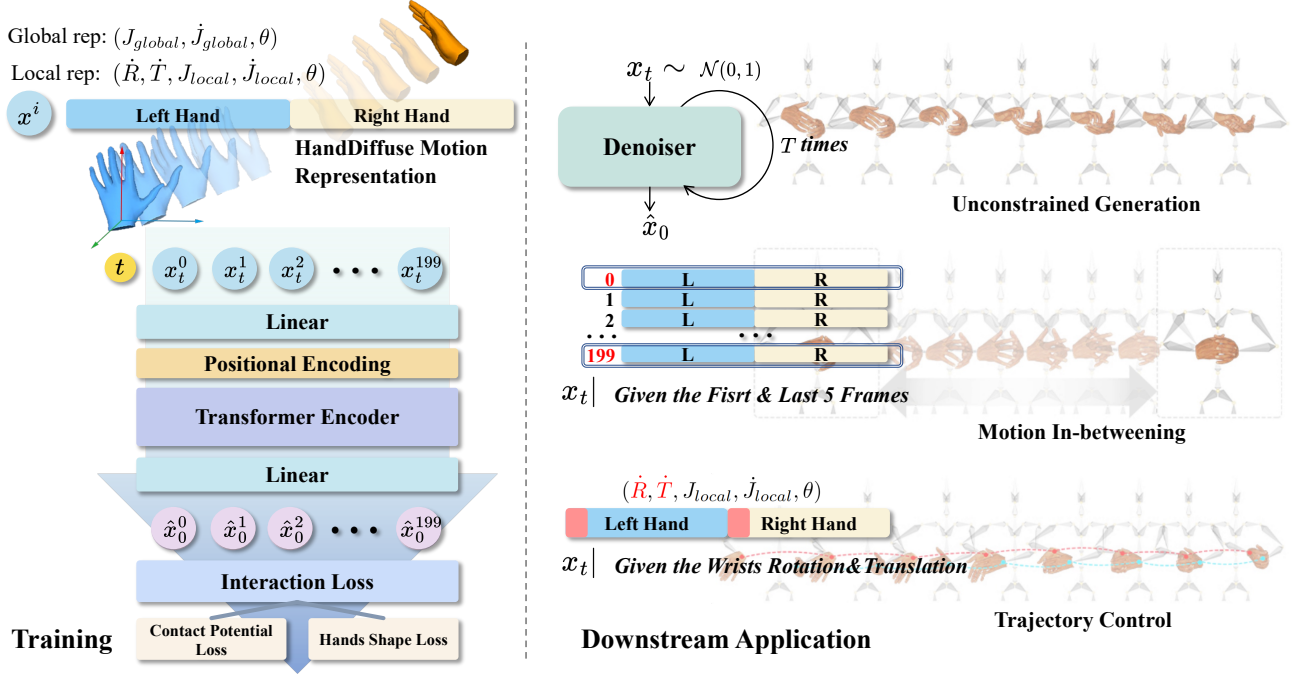


Figure 4. **(Left) HandDiffuse Training procedure overview.** Given HandDiffuse Motion Representation $x_t^{1:N}$ of length N together with a timestep embedding t as input, we use a transformer Encoder to predict the final hand motion $\hat{x}_0^{1:N}$. The proposed Interaction Loss is utilized to regulate the generated motion. **(Right) Downstream Applications overview.** For Unconstrained Generation, we sample pure Gaussian noise x_t and predict the final motion \hat{x}_0 . For Motion In-betweening, we sample the final motion \hat{x}_0 given $x_t^{1:5}$ and $x_t^{-5:N}$. For Trajectory Control, we sample the final motion \hat{x}_0 given the root angular velocity and linear velocity.

adjust the resolution to 3840×2160 to allocate more pixels for capturing hand movements. To ensure uniform illumination and minimize motion blur, we utilize 35 directional LED panel lights and set the shutter speed to $1/500$. We design four categories of hand interaction motions for recording: random and complex hand interactions, hand movements during daily communication, finger tutting dance, and Chinese daily sign language. Each motion sequence is controlled to last approximately one minute.

3.2. 2/3D joint coordinates & MANO fitting

Upon securing multi-view video sequences, Mediapipe [12] is utilized for 2D joint detection with a confidence threshold set at 0.95 to eliminate poorly captured points. The subsequent triangulation of these 2D keypoints yields 3D joint positions in world coordinates, which are then integrated into the MANO 3D hand model [44] which is differentiable and can generate 3D hand mesh from 3D pose and shape inputs. It transforms shape parameters $\beta \in \mathbb{R}^B$, global pose $\theta_g \in \mathbb{R}^3$, and local pose $\theta_l \in \mathbb{R}^{45}$ into vertices $\mathcal{V}_{MANO} \in \mathbb{R}^{D_V \times 3}$ and joints $\mathcal{J}_{MANO} \in \mathbb{R}^{D_J \times 3}$. Here, B denotes the dimensionality of shape parameters, D_V the number of vertices, and D_J the number of hand joints.

To address the computational challenges posed by the full MANO model, which operates with a complexity

of $O(BD_V D_J)$. We developed a compressed MANO model. This model reduces the computational complexity to $O(BD_J)$ by focusing only on the joints' positions. The efficiency is achieved by preprocessing MANO's shape basis to formulate a "joint shape basis", enabling accurate hand pose depiction with fewer computations.

In the optimization phase, we aim to precisely adjust the MANO parameters $(\beta, \theta_g, \theta_l)$ for alignment with the captured 3D joint data. The joint positions as determined by the MANO model are represented as $J_{mano}(\beta, \theta_g, \theta_l)$, while the ground-truth positions are denoted as J_{gt} . The optimization encompasses two primary components:

$$L_{joint} = \|J_{gt} - J_{mano}(\beta, \theta_g, \theta_l)\|_2,$$

$$L_{pose} = \|\theta_l\|^2,$$

$$L_{total} = L_{joint} + \lambda L_{pose},$$

In this formulation, $\lambda > 0$ is a hyperparameter that helps balance joint positioning accuracy with pose regularization.

Despite these steps, errors caused by hand occlusion are still inevitable. We manually verify each frame and annotate erroneous frames for accuracy. For each frame, we choose the six least occluded viewpoints for precise joint position annotation, totaling 240,000 pictures manually annotated. Further information about the construction of the HandDiffuse dataset and the application of the compressed MANO

model for efficient parameter fitting is detailed in the Appendix.

3.3. Quantitative Evaluation for our Dataset.

Table 1 presents a comparison with two existing 3D hand datasets. Our dual-hand dataset focuses on close-hand interactions and temporal sequences. Our HandDiffuse dataset has the highest number of frames, with each sequence containing at least 200 frames. Our HandDiffuse dataset has more than 250,000 temporal frames, making it the largest known dataset of continuous temporal frames for dual-hand interaction data. We anticipate that this dataset with long sequences of close hand interactions will assist in fine-grained hands motion generation. More details are provided in the Appendix.

We evaluate the superiority of our dataset in terms of interaction data diversity and effectiveness. To this end, we compare our dataset with InterHand2.6M [36] and Re:InterHand [37], both of which also contain hand interaction motion sequences. Figure 3 illustrates that our dataset exhibits a greater variety of interaction poses compared to InterHand2.6M and Re:InterHand. This is attributed to our dataset’s explicit focus on hand interaction pose sequences for generation tasks.

4. Method

An overview of our method is shown in Figure 4. With our dataset, the goal is to synthesize two hands motion $\mathbf{x}^{1:N}$ without or with two designed controllers c . These two selected controllers are common in human motion generation and are also able to dictate the synthesis of two hand motions, such as initial and end frames (motion in-betweening) and the positions and rotations of both wrists (trajectory control). In contrast to single-person human motion generation, the task of generating dual-hand motion requires the network to learn not only the local motion of each hand but also the dynamic process of interaction. Therefore, we propose two specific hand motion representations for different controllers 4.1 and Interaction Loss 4.2 to model this dynamic interaction process.

Inspired by recent work, we adopt the diffusion model as the backbone which has shown remarkable generative ability in image generation and human motion generation. Diffuse is modeled as a Markov noising process and the ground truth $\mathbf{x}_0^{1:N}$ is diffused to $\mathbf{x}_t^{1:N}$ by adding t-step independent Gaussian noise $\epsilon \sim \mathcal{N}(0, I)$. This process can be formulated as

$$q(\mathbf{x}_t|\mathbf{x}_0) = \sqrt{\bar{\alpha}_t}\mathbf{x}_0 + (1 - \bar{\alpha}_t),$$

where $\bar{\alpha}_t = \prod_{s=0}^t \alpha_s$ and $\alpha_t = 1 - \beta_t$. β_t is the cosine noise variance schedule and $q(\mathbf{x}_t)$ is near $\mathcal{N}(0, I)$ when t is big enough. Then, \mathbf{x}_t is sent to a denoiser conditioned on

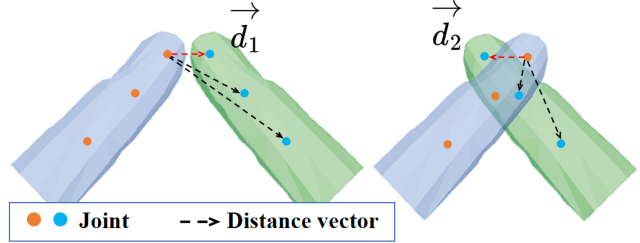


Figure 5. Module of contact potential loss in Interaction Loss. The distance between joints has direction. Despite the approximate similarity in length of \vec{d}_1 and \vec{d}_2 , their directions are opposite. Therefore, it is necessary to consider both the length and direction simultaneously to eliminate ambiguity.

timestep t and different conditions c to predict $\hat{\mathbf{x}}_0$:

$$\hat{\mathbf{x}}_0 = \mathcal{G}(\mathbf{x}_t, t, c).$$

We use an encoder-only transformer to construct our denoiser D following MDM[51] and we concatenate the left hand and right hand together as input.

4.1. Motion representation for two hands.

For different tasks, we have proposed two specific motion representation methods, which we refer to as local representation (local rep) and global representation (global rep). The local rep is inspired by HumanML3D[14], a widely used approach in human motion generation. In each frame, the pose of left hand is defined by a tuple of $(\hat{R}, \hat{T}, J_{local}, \dot{J}_{local}, \theta)$ and the right hand is $(R_{init}, T_{init}, \hat{R}, \hat{T}, J_{local}, \dot{J}_{local}, \theta)$, where $\hat{R} \in \mathbb{R}^4$ and $\hat{T} \in \mathbb{R}^3$ represent root angular velocity in quaternion and linear velocity respectively. $J_{local} \in \mathbb{R}^{3j}$ and $\dot{J}_{local} \in \mathbb{R}^{3j}$ denote the local joint positions and velocities in root space, with $j = 21$ represents the number of joints. $\theta \in \mathbb{R}^{4i}$ represents the local joint rotations in quaternion representation, following the skeleton structure of MANO with $i = 15$. Each sequence is aligned with the left wrist of the first frame as the coordinate system origin. Both left and right hands are rotated to align the left-hand R vector with the direction $(1, 0, 0)$ which is shown in Figure 4. Therefore, the right hand has $R_{init} \in \mathbb{R}^4$ and $T_{init} \in \mathbb{R}^3$.

On the other hand, the global rep is defined as a tuple of $(J_{global}, \dot{J}_{global}, \theta)$ for both hands, where J_{global} represents the positions of hand joints in the world coordinate system and two hands are normalized by employing the same approach as local rep.

During the experimental process, we observed that the local rep performed better in the task of trajectory control, where the global rotation and translation of the hand are given. The global rep achieved better results in the unconditional generation and motion in-betweening tasks. In Sec-

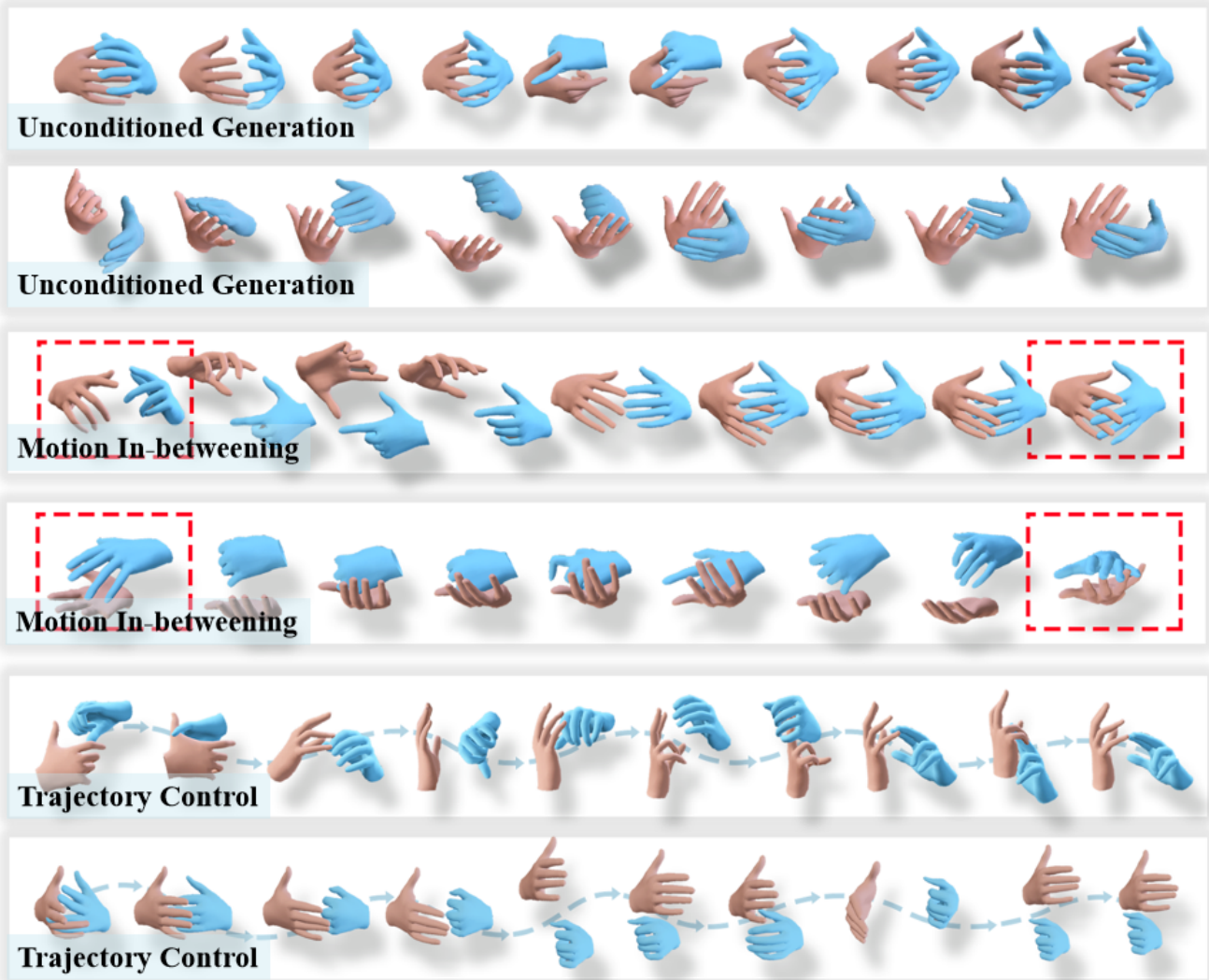


Figure 6. **The Downstream Application of HandDiffuse.** The generation results of downstream applications of HandDiffuse. The generated dual-hand motion exhibits natural and realistic hand interaction.

tion 5.3, a detailed comparison between the two representations is provided.

4.2. Interaction Loss.

The first part of the Interaction Loss is the dual-hand joint contact potential loss. In each frame, we first calculate a 25×25 distance matrix \mathbf{D} between the 21 left-hand joints and 21 right-hand joints with 4 more joints sampled in each palm. Since the interaction between the hands involves fine-grained movements, we should focus on situations where the finger joints are very close to each other. Inspired by the concept of Contact Potential Field[56], we further represent the distances using the elastic potential energy of a spring model and it can be described as

$$Potential = 1/2K \text{relu}(\tau - \|\mathbf{D}_{pred}\|_2)^2, \quad (1)$$

where \mathbf{K} represents the coefficient of elasticity and τ denotes the distance threshold. The closer the distance between the finger joints, the larger the potential energy obtained, and the distance will be filtered out when it is over the threshold. Moreover, by considering the direction of the distance, we can avoid ambiguity caused by penetration, and the final contact potential loss is described as

$$Loss_{potential} = |\mathbf{P}_{pred} - \mathbf{P}_{gt}|(1 + \overrightarrow{\mathbf{D}}_{pred} \times \overrightarrow{\mathbf{D}}_{gt}), \quad (2)$$

where (\times) means cross product. More is shown in Figure 5.

During our testing process, we observed that MANO has strict requirements for the proportional lengths of hand bones. Therefore, the second part of the Interaction Loss is the Shape Loss. We ensure the rationality of hand shape by calculating the differences in bone lengths between the left

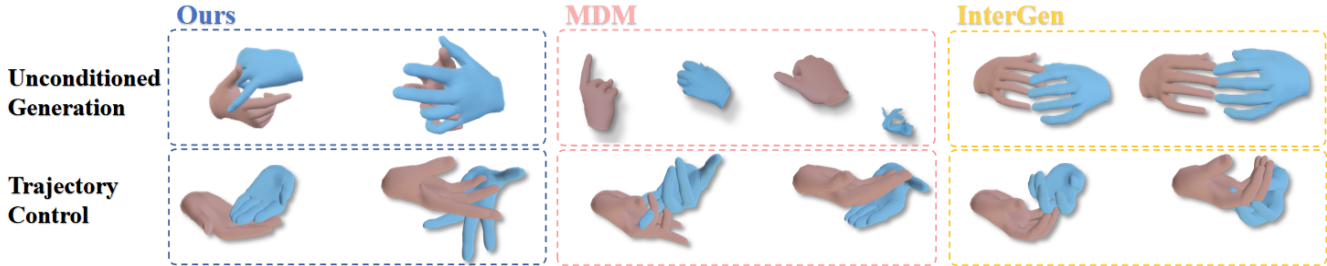


Figure 7. **Qualitative comparison for different methods.** For Unconstrained Generation, MDM[52] tend to generate motion with hands shifting away from each other, while InterGen[31] would generate motions with a mean pose. In terms of Trajectory Control, MDM yields satisfactory results, whereas InterGen generates motion without incorporating interaction.

and right hands, as well as the differences between the predicted shape and the ground truth (GT). This is described as follows:

$$\text{Loss}_{\text{shape}} = |\text{BL}_{\text{left}} - \text{BL}_{\text{right}}| + |\text{BL}_{\text{pred}} - \text{BL}_{\text{GT}}|, \quad (3)$$

where BL denotes the Euclidean distance of the bones.

4.3. Downstream Application

For the task of unconstrained generation and motion in-betweening, the key challenge lies in constructing the global information of the dynamic interaction process between the two hands. Therefore, we choose to use the global rep. In motion in-betweening task, we provide the ground truth for the previous five frames $\mathbf{x}_0^{1:5}$ and the last five frames $\mathbf{x}_0^{-5:-1}$ for the diffused motion $\mathbf{x}_t^{1:N}$.

For the task of trajectory control, the goal is to generate the reasonable local motion given the global rotation and translation of both hands. In this case, using the local rep allows the network to focus on the local motion during the interaction process. Furthermore, we provide $\dot{R}^{1:N}$ and $\dot{T}^{1:N}$ for the diffuse $\mathbf{x}_t^{1:N}$.

5. Experiment

In this section, we conduct several experiments to evaluate our dataset and method for dual-hand motion generation tasks. We particularly evaluate (1) the comparison of our method against previous state-of-the-art approaches, (2) the ability of our method to augment existing datasets, and (3) the effectiveness of our hand motion representation and Interaction Loss. The above evaluations are conducted specifically on the three tasks mentioned in Section 4.3. The models have been trained with $T = 1000$ noising steps and a cosine noise schedule. All of them have been trained on a single *NVIDIA GeForce RTX 3080* GPU for about two days.

5.1. Comparisons of different methods

To the best of our knowledge, our proposed method is the first to specifically target hand-only interaction motion generation. To provide a comprehensive evaluation, we com-

Methods	Unconstrained		In-betweening		Trajectory Control	
	FID↓	Diversity↑	FID↓	Diversity↑	FID↓	Diversity↑
Real	0.050	12.034				
MDM[52]	0.526	10.366	0.616	10.258	0.205	11.265
InterGen[31]	0.251	4.928	0.269	5.385	0.402	9.102
Ours	0.176	11.786	0.282	11.533	0.182	11.523

Table 2. **Quantitative comparisons** of different methods. We compare the **FID** and **Diversity** for different methods. '↓' indicates that results are better with lower metrics. **Bold** means the best result.

pare our approach with two recent state-of-the-art human motion generation methods, namely MDM [52] and InterGen [31]. We modify these methods by adapting their motion representation to enable hand motion generation. As depicted in Figure 7, both MDM and InterGen exhibit limitations when generating hand motion. They tend to produce motion sequences with severe joint penetration or unnatural interaction since they were not originally designed for dual-hand motion generation. In contrast, our proposed method showcases superior performance as demonstrated by the lowest Fréchet Inception Distance (FID) values, as shown in Table 2. The way we adopted to calculate FID is introduced in the Appendix.

5.2. Cross Datasets Evaluation

To evaluate our method cross datasets, we conduct experiments on two large-scale dual-hand interaction motion datasets, InterHand2.6M[36] and Re:InterHand [37] by sampling control signal from these two datasets. As shown in Figure 8, given the first frame and last frame from InterHand2.6M, our model is able to generate diverse motions. Furthermore, Table 3 shows that after performing In-betweening and Trajectory Control tasks on the datasets, the generated data can increase the diversity. This demonstrates the effectiveness of our approach and HandDiffuse can contribute to data augmentation for other datasets. More results and the details of experiments are introduced in the Appendix.

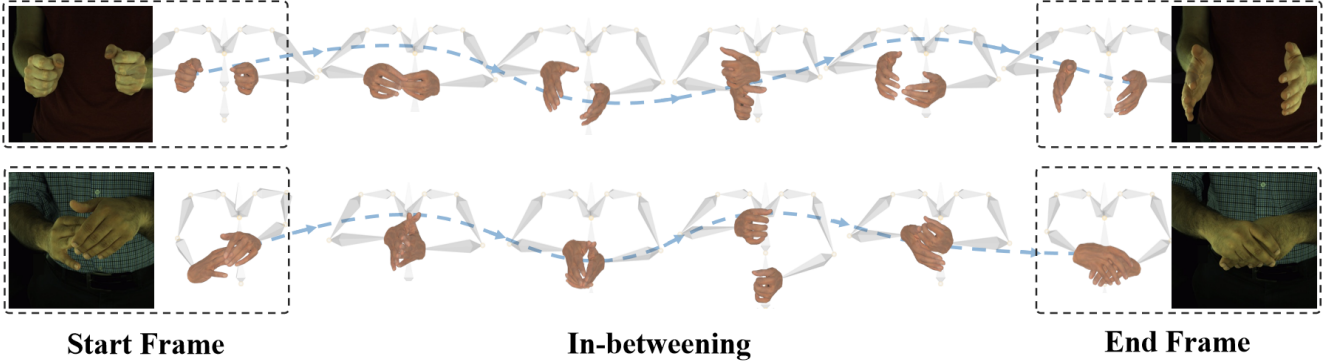


Figure 8. **Cross data Evaluation.** Motion In-betweening task result on InterHand2.6M[36]. We sample two frames in InterHand2.6M as the start frame and end frame and generate the in-betweening motion. Our HandDiffuse can help augment the existing datasets.

Datasets	InterHand		Re:InterHand	
	FID↓	Diversity↑	FID↓	Diversity↑
Real	0.113	8.478	0.034	10.583
In-betweening	0.194	8.171	0.208	11.200
Root Control	0.142	10.146	0.236	12.979

Table 3. **Cross Dataset Evaluation.** The **FID** and **Diversity** both increase, indicating that we get a larger dataset from the original dataset by performing data generation tasks.

5.3. Ablation Study

As we propose two kinds of hand motion representations in section 4.1, here we demonstrate the effectiveness of the representations in different tasks by conducting qualitative and quantitative comparisons. Figure 9 illustrates the limitations of the model without Shape Loss and Interaction Loss. By incorporating the Interaction Loss, we mitigate the issue of joint penetration, resulting in improved motion generation quality. To provide a quantitative analysis, we employ **FID** and the penetration metric **sdf loss(SDF)**[23] for evaluation. **SDF** represents the Signed Distance Field, which could be defined as:

$$\phi(x, y, z) = -\min(SDF(x, y, z), 0), \quad (4)$$

where (x, y, z) denotes the position of MANO vertex. According to the definition, when the hand joints penetrate with each other, ϕ would take the positive value while zero otherwise. Using the formulation, we can measure the severity of penetration during the whole motion. Table 4 demonstrates that our model achieves the highest performance when using the proper motion representation and Interaction Loss.

6. Conclusion

We present HandDiffuse12.5M, the largest interacting hands dataset with strong interaction and temporal se-

Tasks	Unconstrained		In-betweening	Trajectory Control
	FID↓	SDF↓	FID↓	FID↓
Real	0.050	1.146	-	-
w Global rep.	0.168	1.575	0.282	0.415
w Local rep.	0.436	1.988	0.572	0.182
w/o Interaction Loss	0.176	1.652	0.318	0.216
Complete model	0.168	1.575	0.282	0.182

Table 4. **Quantitative comparisons** of different hand motion representations and w/o Interaction Loss. **SDF** indicates the **sdf loss** for penetration of joints during the whole motion. Note that the mean of **sdf loss** is only calculated on frames with penetraion.

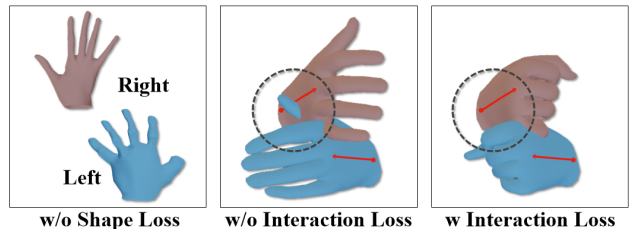


Figure 9. **Ablation Study.** In the absence of Shape Loss, the model generates abnormal hand shapes. Similarly, the absence of Interaction Loss leads to hand interaction motion with severe penetration.

quences, to open up the research direction of interacting hands motion generation. HandDiffuse12.5M consists of various modalities, including synchronous 50-view videos, 3D keypoints and hand poses. Based on HandDiffuse12.5M, we propose a strong baseline method HandDiffuse which is the first interacting hands motion generation approach along with two specific controllers: key frames control and trajectory control. Our evaluation in multi-stage demonstrates the benefit of our approach against others and HandDiffuse fills the blank in human motion generation.

References

- [1] Zhang Baowen, Wang Yangang, Deng Xiaoming, Zhang Yinda, Tan Ping, Ma Cuixia, and Wang Hongan. Interacting two-hand 3d pose and shape reconstruction from single color image. In *International Conference on Computer Vision (ICCV)*, 2021. 3
- [2] Yujun Cai, Yiwei Wang, Yiheng Zhu, Tat-Jen Cham, Jianfei Cai, Junsong Yuan, Jun Liu, Chuanxia Zheng, Sijie Yan, Henghui Ding, et al. A unified 3d human motion synthesis model via conditional variational auto-encoder. In *Proceedings of the IEEE/CVF International Conference on Computer Vision*, pages 11645–11655, 2021. 3
- [3] Yu-Wei Chao, Wei Yang, Yu Xiang, Pavlo Molchanov, Ankur Handa, Jonathan Tremblay, Yashraj S. Narang, Karl Van Wyk, Umar Iqbal, Stan Birchfield, Jan Kautz, and Dieter Fox. DexYCB: A benchmark for capturing hand grasping of objects. In *IEEE/CVF Conference on Computer Vision and Pattern Recognition (CVPR)*, 2021. 2
- [4] Xin Chen, Biao Jiang, Wen Liu, Zilong Huang, Bin Fu, Tao Chen, and Gang Yu. Executing your commands via motion diffusion in latent space. In *Proceedings of the IEEE/CVF Conference on Computer Vision and Pattern Recognition*, pages 18000–18010, 2023. 2
- [5] Zimmermann Christian, Ceylan Duygu, Yang Jimei, Russel Bryan, Argus Max, and Brox Thomas. Freihand: A dataset for markerless capture of hand pose and shape from single rgb images. In *IEEE International Conference on Computer Vision (ICCV)*, 2019. 2
- [6] Xinhan Di and Pengqian Yu. Lwa-hand: Lightweight attention hand for interacting hand reconstruction, 2022. 3
- [7] Yuming Du, Robin Kips, Albert Pumarola, Sebastian Starke, Ali Thabet, and Artsiom Sanakoyeu. Avatars grow legs: Generating smooth human motion from sparse tracking inputs with diffusion model. In *Proceedings of the IEEE/CVF Conference on Computer Vision and Pattern Recognition*, pages 481–490, 2023. 3
- [8] Zicong Fan, Adrian Spurr, Muhammed Kocabas, Siyu Tang, Michael Black, and Otmar Hilliges. Learning to disambiguate strongly interacting hands via probabilistic per-pixel part segmentation. In *International Conference on 3D Vision (3DV)*, 2021. 3
- [9] Zicong Fan, Omid Taheri, Dimitrios Tzionas, Muhammed Kocabas, Manuel Kaufmann, Michael J. Black, and Otmar Hilliges. ARCTIC: A dataset for dexterous bimanual hand-object manipulation. In *Proceedings IEEE Conference on Computer Vision and Pattern Recognition (CVPR)*, 2023. 2
- [10] Daiheng Gao, Yuliang Xiu, Kailin Li, Lixin Yang, Feng Wang, Peng Zhang, Bang Zhang, Cewu Lu, and Ping Tan. DART: Articulated Hand Model with Diverse Accessories and Rich Textures. In *Thirty-sixth Conference on Neural Information Processing Systems Datasets and Benchmarks Track*, 2022. 2
- [11] Guillermo Garcia-Hernando, Shanxin Yuan, Seungryul Baek, and Tae-Kyun Kim. First-person hand action benchmark with rgb-d videos and 3d hand pose annotations. In *Proceedings of Computer Vision and Pattern Recognition (CVPR)*, 2018. 2
- [12] Google. Mediapipe, 2021. 4
- [13] Kristen Grauman, Andrew Westbury, Eugene Byrne, Zachary Chavis, Antonino Furnari, Rohit Girdhar, Jackson Hamburger, Hao Jiang, Miao Liu, Xingyu Liu, Miguel Martin, Tushar Nagarajan, Ilija Radosavovic, Santhosh Kumar Ramakrishnan, Fiona Ryan, Jayant Sharma, Michael Wray, Mengmeng Xu, Eric Zhongcong Xu, Chen Zhao, Siddhant Bansal, Dhruv Batra, Vincent Cartillier, Sean Crane, Tien Do, Morrie Doulaty, Akshay Erapalli, Christoph Feichtenhofer, Adriano Fragomeni, Qichen Fu, Abrahm Gebreselasie, Cristina Gonzalez, James Hillis, Xuhua Huang, Yifei Huang, Wenqi Jia, Weslie Khoo, Jachym Kolar, Satwik Kotur, Anurag Kumar, Federico Landini, Chao Li, Yanghao Li, Zhenqiang Li, Karttikeya Mangalam, Raghava Modhugu, Jonathan Munro, Tullie Murrell, Takumi Nishiyasu, Will Price, Paola Ruiz Puentes, Mery Ramazanova, Leda Sari, Kiran Somasundaram, Audrey Southerland, Yusuke Sugano, Ruijie Tao, Minh Vo, Yuchen Wang, Xindi Wu, Takuma Yagi, Ziwei Zhao, Yunyi Zhu, Pablo Arbelaez, David Crandall, Dima Damen, Giovanni Maria Farinella, Christian Fuegen, Bernard Ghanem, Vamsi Krishna Ithapu, C. V. Jawahar, Hanbyul Joo, Kris Kitani, Haizhou Li, Richard Newcombe, Aude Oliva, Hyun Soo Park, James M. Rehg, Yoichi Sato, Jianbo Shi, Mike Zheng Shou, Antonio Torralba, Lorenzo Torresani, Mingfei Yan, and Jitendra Malik. Ego4d: Around the world in 3,000 hours of egocentric video, 2022. 2
- [14] Chuan Guo, Shihao Zou, Xinxin Zuo, Sen Wang, Wei Ji, Xingyu Li, and Li Cheng. Generating diverse and natural 3d human motions from text. In *Proceedings of the IEEE/CVF Conference on Computer Vision and Pattern Recognition (CVPR)*, pages 5152–5161, 2022. 5
- [15] Shreyas Hampali, Mahdi Rad, Markus Oberweger, and Vincent Lepetit. Honnotate: A method for 3d annotation of hand and object poses. In *CVPR*, 2020. 2
- [16] Shreyas Hampali, Sayan Deb Sarkar, Mahdi Rad, and Vincent Lepetit. Keypoint transformer: Solving joint identification in challenging hands and object interactions for accurate 3d pose estimation. In *IEEE Computer Vision and Pattern Recognition Conference*, 2022. 3
- [17] Shangchen Han, Beibei Liu, Randi Cabezas, Christopher Twigg, Peizhao Zhang, Jeff Petkau, Tsz-Ho Yu, Chun-Jung Tai, Muzaffer Akbay, Zheng Wang, Asaf Nitzan, Gang Dong, Yuting Ye, Lingling Tao, Chengde Wan, and Robert Wang. Megatrack: monochrome egocentric articulated hand-tracking for virtual reality. *ACM Transactions on Graphics*, 39, 2020. 2
- [18] Joo Hanbyul, Liu Hao, Tan Lei, Gui Lin, Nabbe Bart, Matthews Iain, Kanad Takeo, Nobuhara Shohei, and Sheikh Yaser. Panoptic studio: A massively multiview system for social motion capture. 2015. 2
- [19] Meng Hao, Jin Sheng, Liu Wentao, Qian Chen, Lin Mengxiang, Ouyang Wanli, and Luo Ping. 3d interacting hand pose estimation by hand de-occlusion and removal. 2022. 3
- [20] Félix G. Harvey, Mike Yurick, Derek Nowrouzezahrai, and Christopher Pal. Robust motion in-betweening. *ACM Transactions on Graphics*, 39(4), 2020. 3
- [21] Jonathan Ho, Ajay Jain, and Pieter Abbeel. Denoising diffu-

- sion probabilistic models. *Advances in Neural Information Processing Systems*, 33:6840–6851, 2020. 2, 3
- [22] Biao Jiang, Xin Chen, Wen Liu, Jingyi Yu, Gang Yu, and Tao Chen. Motiongpt: Human motion as a foreign language. *arXiv preprint arXiv:2306.14795*, 2023. 2
- [23] Wen Jiang, Nikos Kolotouros, Georgios Pavlakos, Xiaowei Zhou, and Kostas Daniilidis. Coherent reconstruction of multiple humans from a single image. In *Proceedings of the IEEE/CVF Conference on Computer Vision and Pattern Recognition*, pages 5579–5588, 2020. 8
- [24] Korrawe Karunratanakul, Konpat Preechakul, Supasorn Suwajanakorn, and Siyu Tang. Gmd: Controllable human motion synthesis via guided diffusion models. *arXiv preprint arXiv:2305.12577*, 2023. 3
- [25] Manuel Kaufmann, Emre Aksan, Jie Song, Fabrizio Pece, Remo Ziegler, and Otmar Hilliges. Convolutional autoencoders for human motion infilling. In *2020 International Conference on 3D Vision (3DV)*. IEEE, 2020. 3
- [26] Dong Uk Kim, Kwang In Kim, and Seungryul Baek. End-to-end detection and pose estimation of two interacting hands. In *2021 IEEE/CVF International Conference on Computer Vision (ICCV)*, pages 11169–11178, 2021. 3
- [27] Taein Kwon, Bugra Tekin, Jan Stühmer, Federica Bogo, and Marc Pollefeys. H2o: Two hands manipulating objects for first person interaction recognition. In *Proceedings of the IEEE/CVF International Conference on Computer Vision (ICCV)*, pages 10138–10148, 2021. 2
- [28] Lijun Li, Linrui Tian, Xindi Zhang, Qi Wang, Bang Zhang, Mengyuan Liu, and Chen Chen. Renderih: A large-scale synthetic dataset for 3d interacting hand pose estimation. *arXiv preprint arXiv:2309.09301*, 2023. 2, 3
- [29] Lijun Li, Li’an Zhuo, Bang Zhang, Liefeng Bo, and Chen Chen. Diffhand: End-to-end hand mesh reconstruction via diffusion models, 2023. 3
- [30] Mengcheng Li, Liang An, Hongwen Zhang, Lianpeng Wu, Feng Chen, Tao Yu, and Yebin Liu. Interacting attention graph for single image two-hand reconstruction. In *2022 IEEE/CVF Conference on Computer Vision and Pattern Recognition (CVPR)*, pages 2751–2760, 2022. 3
- [31] Han Liang, Wenqian Zhang, Wenxuan Li, Jingyi Yu, and Lan Xu. Intergen: Diffusion-based multi-human motion generation under complex interactions. *arXiv preprint arXiv:2304.05684*, 2023. 2, 3, 7
- [32] Fanqing Lin, Connor Wilhelm, and Tony Martinez. Two-hand global 3d pose estimation using monocular rgb. In *Proceedings of the IEEE/CVF Winter Conference on Applications of Computer Vision (WACV)*, pages 2373–2381, 2021. 2
- [33] Xiao Lin and Mohamed R Amer. Human motion modeling using dv-gans. *arXiv preprint arXiv:1804.10652*, 2018. 3
- [34] Yunze Liu, Yun Liu, Che Jiang, Kangbo Lyu, Weikang Wan, Hao Shen, Boqiang Liang, Zhoujie Fu, He Wang, and Li Yi. Hoi4d: A 4d egocentric dataset for category-level human-object interaction. In *Proceedings of the IEEE/CVF Conference on Computer Vision and Pattern Recognition (CVPR)*, pages 21013–21022, 2022. 2
- [35] Gyeongsik Moon. Bringing inputs to shared domains for 3D interacting hands recovery in the wild. In *CVPR*, 2023. 3
- [36] Gyeongsik Moon, Shoou-I Yu, He Wen, Takaaki Shiratori, and Kyoung Mu Lee. Interhand2.6m: A dataset and baseline for 3d interacting hand pose estimation from a single rgb image. In *European Conference on Computer Vision (ECCV)*, 2020. 2, 3, 5, 7, 8, 12
- [37] Gyeongsik Moon, Shunsuke Saito, Weipeng Xu, Rohan Joshi, Julia Buffalini, Harley Bellan, Nicholas Rosen, Jesse Richardson, Mize Mallorie, Philippe Bree, Tomas Simon, Bo Peng, Shubham Garg, Kevyn McPhail, and Takaaki Shiratori. A dataset of relighted 3D interacting hands. In *NeurIPS Track on Datasets and Benchmarks*, 2023. 2, 3, 5, 7
- [38] JoonKyu Park, Daniel Sungho Jung, Gyeongsik Moon, and Kyoung Mu Lee. Extract-and-adaptation network for 3d interacting hand mesh recovery, 2023. 3
- [39] Georgios Pavlakos, Vasileios Choutas, Nima Ghorbani, Timo Bolkart, Ahmed A. A. Osman, Dimitrios Tzionas, and Michael J. Black. Expressive body capture: 3d hands, face, and body from a single image. In *Proceedings of the IEEE/CVF Conference on Computer Vision and Pattern Recognition (CVPR)*, 2019. 3
- [40] Georgios Pavlakos, Vasileios Choutas, Nima Ghorbani, Timo Bolkart, Ahmed A. A. Osman, Dimitrios Tzionas, and Michael J. Black. Expressive body capture: 3d hands, face, and body from a single image. In *Proceedings IEEE Conf. on Computer Vision and Pattern Recognition (CVPR)*, 2019. 2
- [41] Mathis Petrovich, Michael J Black, and Gül Varol. Action-conditioned 3d human motion synthesis with transformer vae. In *Proceedings of the IEEE/CVF International Conference on Computer Vision*, pages 10985–10995, 2021. 3
- [42] Jia Qin, Youyi Zheng, and Kun Zhou. Motion in-betweening via two-stage transformers. *ACM Transactions on Graphics (TOG)*, 41(6):1–16, 2022. 3
- [43] Davis Rempe, Zhengyi Luo, Xue Bin Peng, Ye Yuan, Kris Kitani, Karsten Kreis, Sanja Fidler, and Or Litany. Trace and pace: Controllable pedestrian animation via guided trajectory diffusion. In *Proceedings of the IEEE/CVF Conference on Computer Vision and Pattern Recognition (CVPR)*, pages 13756–13766, 2023. 3
- [44] Javier Romero, Dimitrios Tzionas, and Michael J. Black. Embodied hands: Modeling and capturing hands and bodies together. *ACM Transactions on Graphics, (Proc. SIGGRAPH Asia)*, 36(6), 2017. 3, 4
- [45] Yu Rong, Jingbo Wang, Ziwei Liu, and Chen Change Loy. Monocular 3d reconstruction of interacting hands via collision-aware factorized refinements. In *International Conference on 3D Vision*, 2021. 3
- [46] Olaf Ronneberger, Philipp Fischer, and Thomas Brox. U-net: Convolutional networks for biomedical image segmentation, 2015. 3
- [47] F. Sener, D. Chatterjee, D. Shelepov, K. He, D. Singhania, R. Wang, and A. Yao. Assembly101: A large-scale multi-view video dataset for understanding procedural activities. *CVPR 2022*, 2022. 2
- [48] Tomas Simon, Hanbyul Joo, Iain Matthews, and Yaser Sheikh. Hand keypoint detection in single images using multiview bootstrapping. In *Proceedings of the IEEE Conference*

- on *Computer Vision and Pattern Recognition (CVPR)*, 2017. 2
- [49] Jiaming Song, Chenlin Meng, and Stefano Ermon. Denoising diffusion implicit models. *arXiv preprint arXiv:2010.02502*, 2020. 3
- [50] Guy Tevet, Brian Gordon, Amir Hertz, Amit H Bermano, and Daniel Cohen-Or. Motionclip: Exposing human motion generation to clip space. *arXiv preprint arXiv:2203.08063*, 2022. 12, 13
- [51] Guy Tevet, Sigal Raab, Brian Gordon, Yonatan Shafir, Amit H Bermano, and Daniel Cohen-Or. Human motion diffusion model. *arXiv preprint arXiv:2209.14916*, 2022. 2, 5, 12
- [52] Guy Tevet, Sigal Raab, Brian Gordon, Yoni Shafir, Daniel Cohen-or, and Amit Haim Bermano. Human motion diffusion model. In *The Eleventh International Conference on Learning Representations*, 2023. 3, 7
- [53] Dimitrios Tzionas, Luca Ballan, Abhilash Srikantha, Pablo Aponte, Marc Pollefeys, and Juergen Gall. Capturing hands in action using discriminative salient points and physics simulation. *International Journal of Computer Vision (IJCV)*, 2016. 2
- [54] Yiming Xie, Varun Jampani, Lei Zhong, Deqing Sun, and Huaizu Jiang. Omnicontrol: Control any joint at any time for human motion generation. *arXiv preprint arXiv:2310.08580*, 2023. 3
- [55] Sijie Yan, Zhizhong Li, Yuanjun Xiong, Huahan Yan, and Dahua Lin. Convolutional sequence generation for skeleton-based action synthesis. In *Proceedings of the IEEE/CVF International Conference on Computer Vision*, pages 4394–4402, 2019. 3
- [56] Lixin Yang, Xinyu Zhan, Kailin Li, Wenqiang Xu, Jiefeng Li, and Cewu Lu. Cpf: Learning a contact potential field to model the hand-object interaction. In *ICCV*, 2021. 6
- [57] Zhixuan Yu, Jae Shin Yoon, In Kyu Lee, Prashanth Venkatesh, Jaesik Park, Jihun Yu, and Hyun Soo Park. Humbi: A large multiview dataset of human body expressions. In *IEEE/CVF Conference on Computer Vision and Pattern Recognition (CVPR)*, 2020. 2
- [58] Jiawei Zhang, Jianbo Jiao, Mingliang Chen, Liangqiong Qu, Xiaobin Xu, and Qingxiong Yang. 3d hand pose tracking and estimation using stereo matching, 2016. 2
- [59] Mingyuan Zhang, Zhongang Cai, Liang Pan, Fangzhou Hong, Xinying Guo, Lei Yang, and Ziwei Liu. Motiondiffuse: Text-driven human motion generation with diffusion model. *arXiv preprint arXiv:2208.15001*, 2022. 2
- [60] Siwei Zhang, Yan Zhang, Federica Bogo, Marc Pollefeys, and Siyu Tang. Learning motion priors for 4d human body capture in 3d scenes. In *Proceedings of the IEEE/CVF International Conference on Computer Vision (ICCV)*, pages 11343–11353, 2021. 3
- [61] Siwei Zhang, Qianli Ma, Yan Zhang, Zhiyin Qian, Taemin Kwon, Marc Pollefeys, Federica Bogo, and Siyu Tang. Ego-body: Human body shape and motion of interacting people from head-mounted devices. In *European Conference on Computer Vision*, pages 180–200. Springer, 2022. 3
- [62] Rui Zhao, Hui Su, and Qiang Ji. Bayesian adversarial human motion synthesis. In *Proceedings of the IEEE/CVF Conference on Computer Vision and Pattern Recognition (CVPR)*, 2020. 3
- [63] Christian Zimmermann and Thomas Brox. Learning to estimate 3d hand pose from single rgb images. Technical report, arXiv:1705.01389, 2017. <https://arxiv.org/abs/1705.01389>. 2
- [64] Binghui Zuo, Zimeng Zhao, Wenqian Sun, Wei Xie, Zhou Xue, and Yangang Wang. Reconstructing interacting hands with interaction prior from monocular images. In *Proceedings of the IEEE/CVF International Conference on Computer Vision*, 2023. 2, 3

Appendix

7. Experiment Details

7.1. Frechet Inception Distance (FID)

The Frechet Inception Distance (FID) is a metric used to quantify the dissimilarity between the distributions of generated and ground truth data in latent space. In our experiments, we employ FID as a crucial indicator to measure the authenticity and plausibility of our generated data. And the formula is

$$FID = |\mu_{gt} - \mu_{gen}|^2 + \text{Tr}(C_{gt} + C_{gen} - 2\sqrt{C_{gt}C_{gen}}),$$

where μ_{gt} and μ_{gen} are the mean feature vectors of ground truth and generated motions, respectively; C_{gt} and C_{gen} are the covariance feature matrices of real and generated motions, respectively; $\text{Tr}(\cdot)$ denotes the trace of the matrix. In the previous works[51], the feature is extracted by a Inception network which is a classifier. However, in the interacting hands datasets, it is challenging to label these complex interactive movements, making it difficult to build a classifier. Therefore, taking inspiration from MotionCLIP[50], we propose a self-supervised encoder-decoder architecture for the reconstruction network, as depicted in Figure 10.

More specifically, we concatenate a z_{tk} vector of equal dimensions to the original motion representation $x^{1:T}$. This concatenated sequence $x^{1:T+1}$ is then fed into a transformer encoder. From the encoder’s output, we select the corresponding position z_x as the feature representation for the input motion segment. This obtained feature z_x serves as the memory for the decoder. Additionally, we use a T-length zero vector that undergoes positional encoding as the target for reconstructing the motion in the decoder. The reconstruction loss is computed using the L2 norm.

During experimentation, we observed that using the global representation of the motion improves the convergence of the network. Therefore, in subsequent experiments, we convert the motion to a global representation before calculating the motion’s feature.

7.2. Diversity

Diversity measures the variability in the resulting motion distribution. The way we followed to calculate Diversity is as same as MDM[51]. We randomly generate 1000 samples and select 200 of them for calculating.

8. HandDiffuse12.5M

Figure 11 has shown the diversity and complexity of our dataset HandDiffuse12.5M. Figure 12 has shown our manual annotation tool.

9. More Results

Figure 13 has shown the results of trajectory control task. In each sequence, we adopt the wrists’ rotation and translation from InterHand2.6M[36] as our control signal and we can generate different motion based on this trajectory.

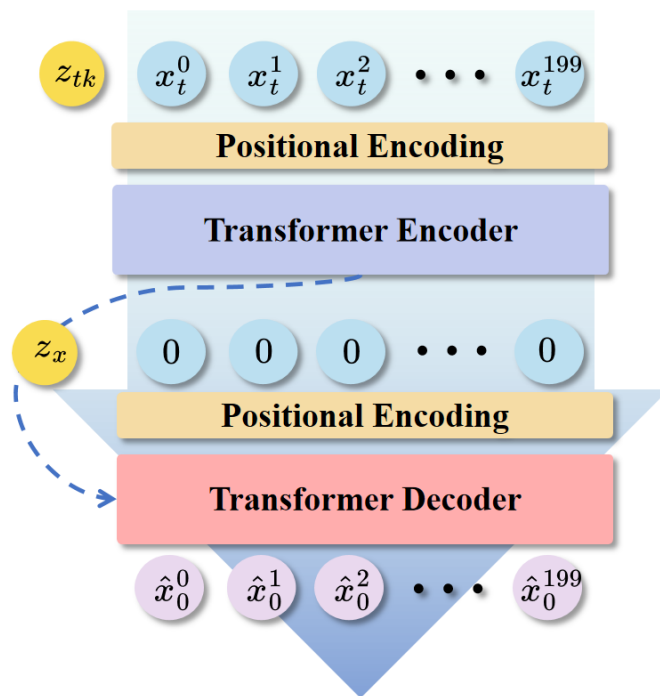


Figure 10. **Feature Extractor for FID.** Inspired by MotionCLIP[50], we train a transformer with encoder-decoder architecture by using self-supervised strategy.

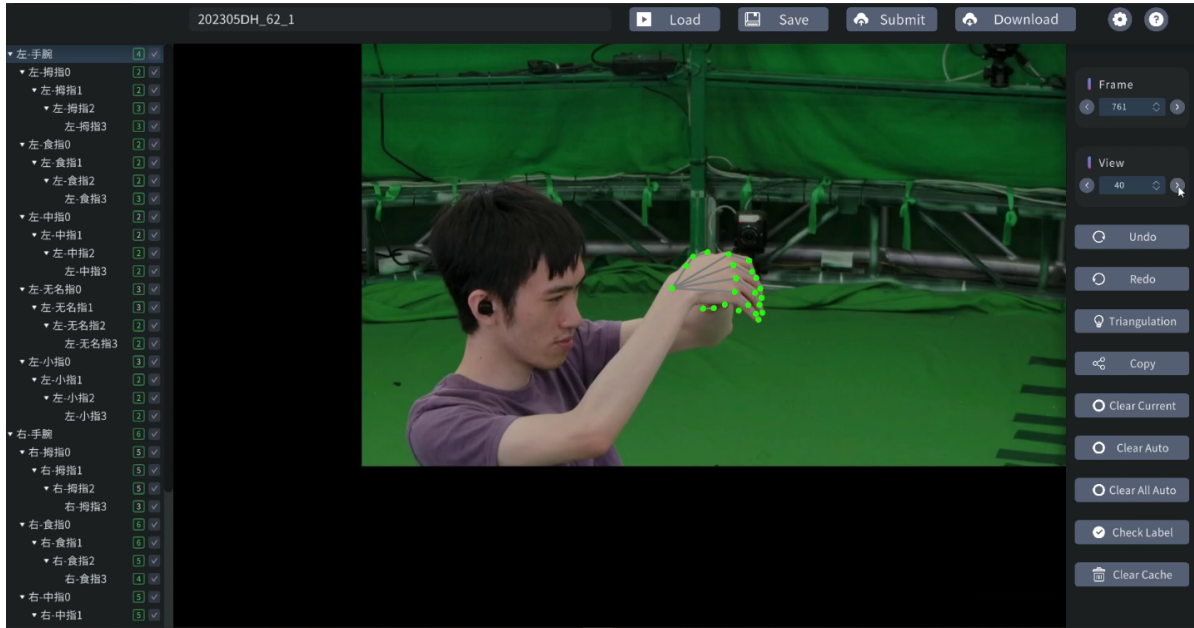


Figure 12. **Annotation Tool**. Our specially designed tool for hand joint annotation of severely occluded frames.

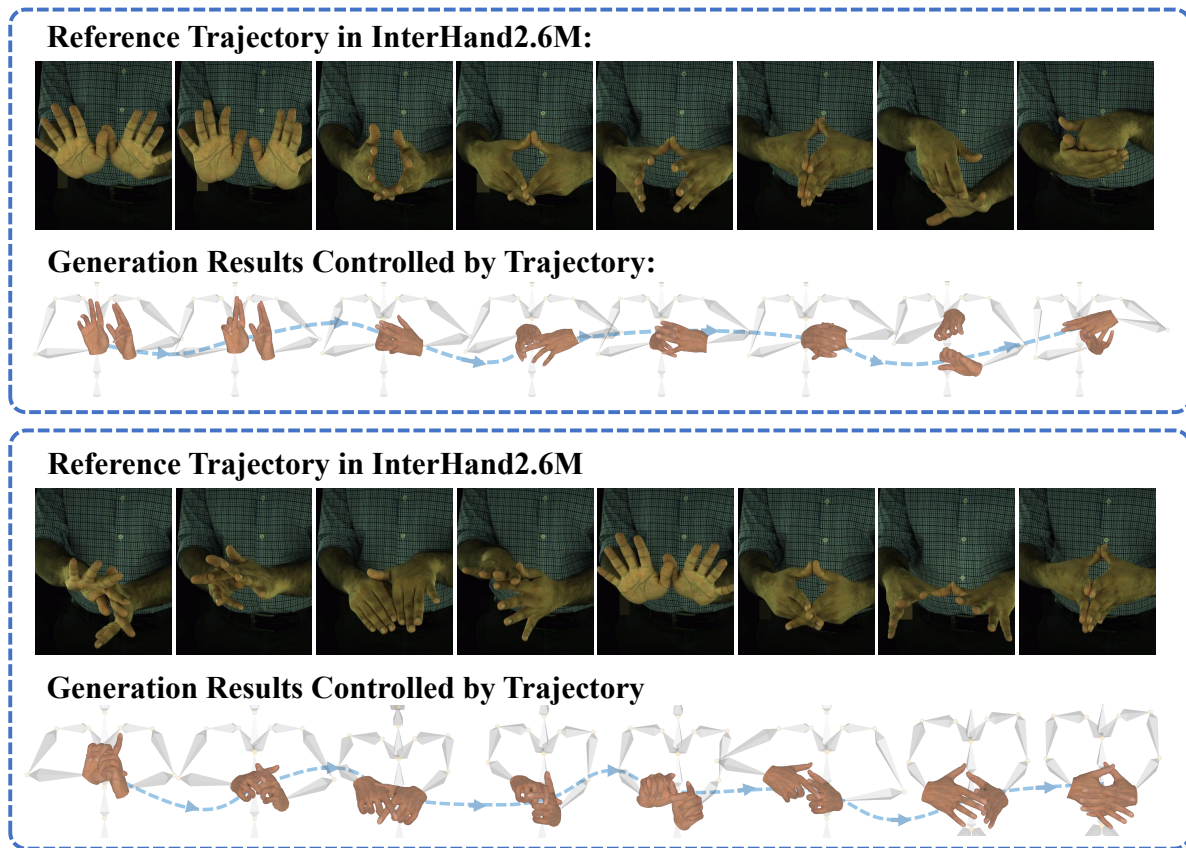


Figure 13. **Results of Trajectory Control by Sampling from InterHand2.6M**. Note that only Root orientation and position is given, the local motions for hand joints are generated from our model.